Automatica 49 (2013) 3425–3431

Contents lists available at ScienceDirect

Automatica

journal homepage: www.elsevier.com/locate/automatica

Brief paper

An impulse-time perturbation approach for enhancing the robustness of extra-insensitive input shapers☆

Keun-Ho Rew [a], Chang-Wan Ha [b], Kyung-Soo Kim [b,1]

[a] Robot-Automation Div., Department of Mechanical Engineering, Hoseo University, Asan-si, Chungnam 336-795, Republic of Korea
[b] Department of Mechanical Engineering, KAIST, 291 Daehak-no, Yuseong-gu, Daejeon 305-701, Republic of Korea

ARTICLE INFO

Article history:
Received 9 April 2012
Received in revised form
14 May 2013
Accepted 24 July 2013
Available online 18 September 2013

Keywords:
Motion control
Input shaping technique
Command shaping
Robust input shaper

ABSTRACT

In this paper, perturbation-based extra-insensitive input shapers (PEI-ISs) are proposed to enhance the robustness of the input shaping technique. The extra-insensitive input shaper (EI-IS) has been known to be more robust than the so-called derivative input shapers such as ZVD, ZVDD, and ZVDDD shapers. However, the robustness of the known EI-IS is restricted by the symmetric property in the sensitivity curve. To address this, the PEI-IS is devised by multiplying a series of input shapers in the Laplace domain, of which the impulse times are slightly perturbed from those of the zero vibration (ZV) shaper. For a single-hump case, a closed-form solution to the PEI-IS is provided. For two- and three-hump cases, the approximate solutions are presented. The robustness is evaluated by simulations and assessed by means of the insensitivity. It will be shown that the proposed PEI-IS does improve the robustness and that it can be easily designed.

1. Introduction

Recently, there has been much effort on generating reference commands with reduced residual vibration or overshoot. The S-curve is one of the well-known methods for smooth motion control (Meckl & Arestides, 1998). Also, elaborate approaches for generating reference commands have been proposed in the literature (Baumgart & Pao, 2007; Ha, Rew, & Kim, 2012; Pao & Singhose, 1998; Rew, Ha, & Kim, 2009; Rew & Kim, 2010).

Together with well-designed motion profiles, in order to achieve fast and accurate motion with less residual vibration, the input shaping technique (IST) has been widely studied in the literature (Diaz, Pereira, Feliu, & Cela, 2010; Pao, Chang, & Hou, 1997; Singer & Seering, 1990; Singhose, Porter, Tuttle, & Singer, 1997). By convolving the reference input signal with a series of impulses, the vibratory mode of the plant can be effectively canceled. During the last couple of decades, thanks to its effectiveness and simplicity, various relevant principles and applications have been reported (Pereira, Trapero, Diaz, & Feliu, 2009; Sorensen & Singhose, 2008).

Since the IST relies on an open loop in general, there exists an issue of robustness against system uncertainties. In particular, it is known that the zero vibration (ZV) input shaper is rather sensitive to the natural frequency variation. To improve the robustness of the IST, there have been several approaches such as the derivative shaper (i.e., ZVD and its extensions) and extra-insensitive input shaper (EI-IS) in the literature (Singhose, Seering, & Singer, 1994). The EI-IS is known to be much more robust than the derivative shaper. In Kang (2011) and Park, Lee, Lim, and Sung (2001), the EI-IS is graphically analyzed in the discrete-time domain using a sensitive curve, and further enhancement of robustness is achieved.

This paper investigates the perturbation-based extra-insensitive input shaper (PEI-IS) in the Laplace domain, which allows the representation of the percent residual vibration (PRV) by a multiplication of input shapers having impulse times slightly perturbed from those of the ZV shaper. Under this framework, the basic idea of this paper starts from the fact that the multiplication of two perturbed input shapers results in a PEI-IS with a single hump allowing an explicit formula. Moreover, the results are extended to present more general cases with two (or three) humps in the sensitivity curve. This paper is organized as follows. In Section 2, the conventional IST is revisited. Then, the impulse-time perturbation approach is newly introduced for deriving PEI-ISs in Section 3. The comparison of robustness is given in Section 4 among several ISTs. Finally, in Section 5, the conclusion follows.

☆ This work was supported by Basic Science Research Program through the National Research Foundation of Korea (NRF) funded by the Korea government (MOE:2011-0010827, MSIP:2013-006603), Korea. The material in this paper was not presented at any conference. This paper was recommended for publication in revised form by Associate Editor Faryar Jabbari under the direction of Editor Roberto Tempo.

E-mail addresses: khrew@hoseo.edu (K.-H. Rew), hawan@kaist.ac.kr (C.-W. Ha), kyungsookim@kaist.ac.kr (K.-S. Kim).

[1] Tel.: +82 42 350 3047.

0005-1098/$ – see front matter © 2013 Elsevier Ltd. All rights reserved.
http://dx.doi.org/10.1016/j.automatica.2013.08.015

2. Preliminaries

Let us consider the second-order linear system

$$G(s) = \frac{\omega_n^2}{s^2 + 2\zeta\omega_n s + \omega_n^2} = \frac{\omega_n^2}{(s - s_p)(s - \bar{s}_p)}, \tag{1}$$

where ω_n and ζ are the natural frequency and the damping ratio, respectively; s_p and its complex conjugate $\bar{s}_p$ are the poles defined by $s_p \triangleq -\zeta\omega_n - j\omega_n\sqrt{1-\zeta^2}$.

The input shaping method convolves the original command with a sequence of impulses. The ZV shaper may be expressed in the Laplace domain as follows (Singer & Seering, 1990):

$$F_0(s) = A_1 + A_2 e^{-\tau_d s}, \tag{2}$$

where $A_1 = \frac{1}{1+K}$, $A_2 = \frac{K}{1+K}$, $\tau_d = \frac{\pi}{\omega_n\sqrt{1-\zeta^2}}$ for $K \triangleq e^{-\pi\zeta/\sqrt{1-\zeta^2}}$. Observe that

$$F_0(s_p) = F_0(\bar{s}_p) = 0, \tag{3}$$

which implies that the input shaper has zeros at s_p and $\bar{s}_p$. This leads to the pole-zero cancellation removing the vibratory mode in the motion control system.

To impose robustness against the natural frequency variation, the ZVD shaper is proposed as follows:

$$F_{\mathrm{ZVD}}(s) = {A_1}^2 + 2A_1A_2e^{-\tau_d s} + {A_2}^2e^{-2\tau_d s}. \tag{4}$$

In general, derivative input shapers can be expressed by $F_{\mathrm{ZVD}^k}(s) = (A_1 + A_2e^{-\tau_d s})^{k+1}$, for $k = 1, 2, 3, \ldots$, and the robustness can be enhanced as k increases. However, the shaping period increases accordingly.

In fact, the robustness of an input shaper has gained attention since the motion profiles are often applied in an open-loop control. In addition to the derivative shapers aforementioned, an extra-insensitive input shaper (EI-IS) was introduced in Singhose et al. (1994) which allows a wider range of natural frequency variation while reducing the residual vibration within a certain level.

3. Main results

3.1. Perturbation-based EI-IS with a single hump

Let us consider two perturbed input shapers as follows: given a design parameter, $0 \le \epsilon < 1$,

$$\begin{cases} F_1(s) \triangleq A_1 + A_2e^{-\tau_d(1-\epsilon)s} \\ F_2(s) \triangleq A_1 + A_2e^{-\tau_d(1+\epsilon)s}, \end{cases} \tag{5}$$

where A_1, A_2, and τ_d are the same as in (2). The two input shapers are obtained by perturbing the impulse time of the ZV shaper in (2). From (3), this leads to

$$F_1\left(\frac{s_p}{1-\epsilon}\right) = F_2\left(\frac{s_p}{1+\epsilon}\right) = 0, \tag{6}$$

which holds at the complex conjugates as well.

Using two perturbed input shapers, let us propose a perturbation-based EI-IS (so-called PEI-IS1) as follows:

$$\begin{aligned} F_{12}(s) &\triangleq F_1(s) \cdot F_2(s) \\ &= A_1^2 + A_1A_2e^{-\tau_d(1-\varepsilon)s} + A_1A_2e^{-\tau_d(1+\varepsilon)s} + A_2^2e^{-2\tau_d s}. \end{aligned} \tag{7}$$

It is noted that the length of the shaping period is equal to that of the ZVD shaper in (4). Also, observe that, as $\epsilon \to 0$, PEI-IS1 approaches the ZVD shaper.

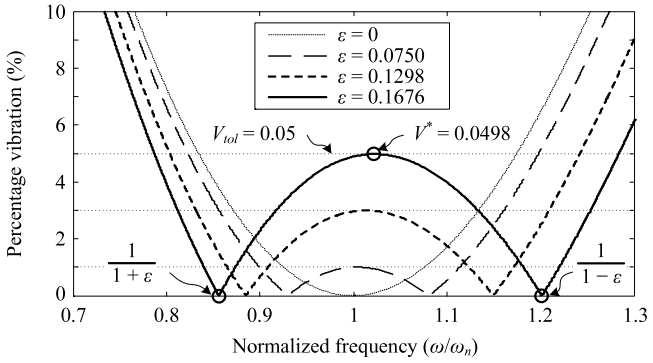

Fig. 1. Sensitivity curves for the PEI-IS with a single hump.

To assess the residual vibration, let us evaluate the percent residual vibration (PRV) introduced by Kozak, Singhose, and Ebert-Uphoff (2006) as follows:

$$\begin{aligned} V &= e^{-\zeta\omega t_4}\left(\left[\sum_{i=1}^{4} A_i \mathrm{Re}\{e^{\omega t_i(\zeta + j\sqrt{1-\zeta^2})}\}\right]^2\right. \\ &\quad \left. + \left[\sum_{i=1}^{4} A_i \mathrm{Im}\{e^{\omega t_i(\zeta + j\sqrt{1-\zeta^2})}\}\right]^2\right)^{1/2} \\ &= e^{-\zeta\omega t_4}\left|\sum_{i=1}^{4} A_i e^{\omega t_i(\zeta + j\sqrt{1-\zeta^2})}\right| \\ &= e^{-\zeta\omega_n t_4(\omega/\omega_n)}\left|\sum_{i=1}^{4} A_i e^{-t_i \cdot s_p(\omega/\omega_n)}\right| \\ &= K^{2\tilde{\omega}}\left|F_{12}\left(s_p\tilde{\omega}\right)\right|, \quad (\because t_4 = 2\tau_d), \end{aligned} \tag{8}$$

where $\tilde{\omega}$ is the normalized natural frequency with respect to the modeled one, ω_n. Hence, without loss of generality, the PRV can be viewed as the function of $\tilde{\omega}$ such that $V(\tilde{\omega}) = K^{2\tilde{\omega}}\left|F_{12}\left(s_p\tilde{\omega}\right)\right|$. (8) shows that the PRV can be expressed by the multiplication of the perturbed input shapers. It leads to an important feature of the PRV such that, from (6),

$$V\left(\frac{1}{1+\epsilon}\right) = V\left(\frac{1}{1-\epsilon}\right) = 0. \tag{9}$$

For a sample system given by $(\zeta, \omega_n) = (0.1, 20\pi)$, several sensitivity curves (such a curve being a plot of the PRV versus frequency) for various values of ϵ are shown in Fig. 1. There exist two notches at $1/(1+\epsilon)$ and $1/(1-\epsilon)$, and a hump between them. Also, the sensitivity curve is not symmetric, in general, so the peak is not exactly located at $\tilde{\omega} = 1$. It is noted that the peak (i.e., V^*) of the hump increases as does ϵ. As a special case, the proposed PEI-IS matches the ZVD shaper when $\epsilon = 0$ (i.e., $V^* = 0$). Similarly, the standard EI-IS approaches the ZVD shaper as $V^* \to 0$.

In Fig. 1, PEI-IS1, given in (7), suppresses the residual vibration less than the peak, V^* (which may be considered as a tolerance), within a range of natural frequency variation. It is noted that V^* depends on the impulse-time perturbation, ϵ. Therefore, the major concern is to derive a relationship between V^* and ϵ in order to determine ϵ for a given tolerance. The result is proposed in the following.

Theorem 1. *For a sufficiently small $\epsilon > 0$, it holds that*

$$V^* = (\sigma\epsilon)^2 + \mathcal{O}(\epsilon^3), \tag{10}$$

where $\sigma \triangleq \frac{\pi A_2}{\sqrt{1-\zeta^2}}$ and V^* is the peak of the hump.

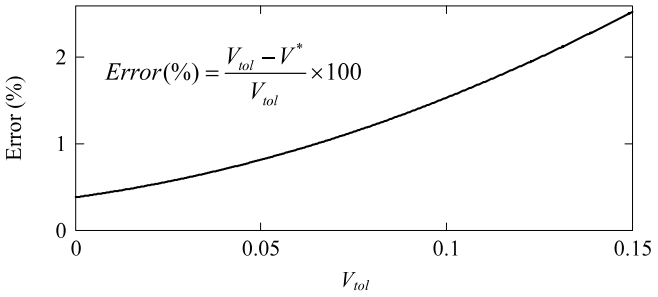

Fig. 2. Accuracy of the PEI-IS with a single hump.

Proof. Recalling the sensitivity curves in Fig. 1, consider that the peak exists near to the center of two notches. Hence, let us approximate the peak such that $V^* \simeq V(\tilde{\omega}_c)$, where $\tilde{\omega}_c = \frac{1}{2}\left(\frac{1}{1+\epsilon} + \frac{1}{1-\epsilon}\right) = \frac{1}{1-\epsilon^2}$. Since $V = K^{2\tilde{\omega}}|F_1(s_p\tilde{\omega})| \cdot |F_2(s_p\tilde{\omega})|$, consider the following.

$$\begin{aligned} F_1(s_p\tilde{\omega}_c) &= A_1 + A_2 e^{-\tau_d s_p \frac{1}{1+\varepsilon}} \\ &= A_2 e^{-\tau_d s_p}\left(-1 + e^{\tau_d s_p \frac{\varepsilon}{1+\varepsilon}}\right) \quad \text{(from (3))} \\ &= A_2 e^{-\tau_d s_p} \cdot \tau_d s_p \varepsilon + \mathcal{O}(\epsilon^2). \end{aligned} \tag{11}$$

In a similar manner, it may be shown that

$$F_2(s_p\tilde{\omega}_c) = -A_2 e^{-\tau_d s_p} \cdot \tau_d s_p \epsilon + \mathcal{O}(\epsilon^2). \tag{12}$$

Moreover, it is easy to show that $K^{2\tilde{\omega}_c} = K^2 + \mathcal{O}(\epsilon^2)$. Considering that $|e^{-\tau_d s_p}| = 1/K$ and $|\tau_d s_p| = \pi/\sqrt{1-\zeta^2}$, we have

$$\begin{aligned} V(\tilde{\omega}_c) &= K^2 \cdot A_2^2 \cdot \frac{1}{K^2} \cdot \left(\pi/\sqrt{1-\zeta^2}\right)^2 \cdot \epsilon^2 + \mathcal{O}(\epsilon^3) \\ &= (\sigma\epsilon)^2 + \mathcal{O}(\epsilon^3). \end{aligned} \tag{13}$$

Since ϵ is sufficiently small, (11)–(13) lead to (10), which completes the proof. □

In fact, Theorem 1 provides an important design rule to select an impulse perturbation, ϵ, for a given tolerance, V_{tol}. To ensure that the peak of the hump, V^*, is smaller than the tolerance, V_{tol}, one may choose ϵ as follows:

$$\epsilon = 0.9981\sqrt{V_{\text{tol}}}/\sigma. \tag{14}$$

It is noted that the scalar value 0.9981 is numerically chosen to meet $V^* \le V_{\text{tol}}$ for all $(\zeta, V_{\text{tol}}) \in [0, 0.3] \times [0, 0.15]$.

To verify the proposition in (14), for the sample system of $(\zeta, \omega_n) = (0.1, 20\pi)$, one may obtain $\epsilon = 0.1676$ from (14) when $V_{\text{tol}} = 0.05$ (i.e., 5% tolerance). Observe that, in Fig. 1, $V^* = 0.0496$, which is minutely smaller than the tolerance. The errors between V^* and V_{tol} are numerically computed for various V_{tol} and plotted in Fig. 2. Observe that the proposition in (14) guarantees that V^* matches very well and is always smaller than V_{tol}. A similar tendency can be observed for various damping ratios.

As a result, PEI-IS1, given in (7), can be easily designed by simply choosing a single parameter, ϵ, based on a closed-form solution (14) with high accuracy, which is a unique advantage of the proposed approach.

3.2. Perturbation-based EI-IS with two humps

To generate two humps in the PRV, let us propose a PEI-IS (so-called PEI-IS2) in the following: for $0 \le \epsilon < 1$,

$$F_{123}(s) \triangleq F_1(s) \cdot F_2(s) \cdot F_3(s). \tag{15}$$

Observe that PEI-IS2 with two humps approaches the ZVDD shaper as $\epsilon \to 0$. Also, the length of the shaping period is the same as that of the ZVDD shaper.

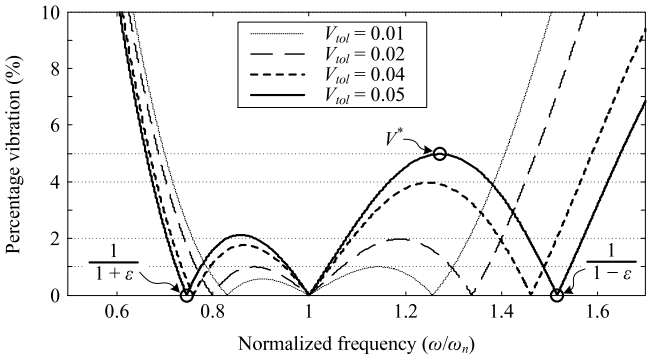

Fig. 3. Sensitivity curves for the PEI-IS with two humps.

The PRV of PEI-IS2 can be expressed by

$$V(\tilde{\omega}) = K^{3\tilde{\omega}}\left|F_{012}(s_p\tilde{\omega})\right|. \tag{16}$$

As illustrated in Fig. 3, the sensitivity curve of the proposed PEI-IS2 should have two humps, since $V\left(\frac{1}{1+\epsilon}\right) = V(1) = V\left(\frac{1}{1-\epsilon}\right) = 0$. So far, the relationship between V^* and ϵ has not been known in an analytic form, differently from the case with a single hump. However, PEI-IS2 can be easily generated by choosing a single design parameter ϵ for a given damping ratio, and the corresponding PRV can be computed to check whether the peak of the hump meets the desired tolerance. Nevertheless, for practical purposes, one may need an explicit representation such that $\epsilon = f(\zeta, V_{\text{tol}})$ even by an approximation as in Singhose et al. (1997). Suppose that ϵ is approximated by

$$\epsilon = [p_{00}, p_{10}, p_{01}, p_{20}, p_{11}, p_{02}, p_{30}, p_{21}, p_{12}, p_{03}] \cdot \varphi^T, \tag{17}$$

where $\varphi \triangleq [1, \zeta, V_{\text{tol}}, \zeta^2, \zeta V_{\text{tol}}, V_{\text{tol}}^2, \zeta^3, \zeta^2 V_{\text{tol}}, \zeta V_{\text{tol}}^2, V_{\text{tol}}^3]$, and the p_{ij} are the coefficients to be determined. For the specific region of $(\zeta, V_{\text{tol}}) \in [0, 0.1] \times [0.01, 0.05]$, we introduce the numerical procedures in the following.

(i) Given a point of $(\zeta, V_{\text{tol}}) \in [0, 0.1] \times [0.01, 0.05]$, find ϵ which achieves the objective function, $J_{2h} = (V_\epsilon^* - V_{\text{tol}})^2$, where V_ϵ^* is the local maximum at $\tilde{\omega} \in [1, \frac{1}{1-\epsilon}]$, to be minimal by using a MATLAB function—fminsearch(·). By repeating the same computation for various points, produce a numerical table of $(\zeta, V_{\text{tol}}, \epsilon)$.

(ii) For the obtained table of $(\zeta, V_{\text{tol}}, \epsilon)$, compute the p_{ij} by fitting the relationship in (17) by using a MATLAB function—sftool(·).

The coefficients p_{ij} obtained by the above procedures are summarized in Table 1. To verify the accuracy of (17), it was obtained, at $\zeta = 0.1$, that $\epsilon = 0.2040, 0.2882$, and 0.3402 for $V_{\text{tol}} = 0.01, 0.03$, and 0.05, respectively. According to these values, the sensitivity curves are shown in Fig. 3. Observe that the peak of the hump is minutely smaller than the tolerance. Over the area of $(\zeta, V_{\text{tol}}) \in [0, 0.1] \times [0.01, 0.05]$, the proposed approximation provides high accuracy.

3.3. Perturbation-based EI-IS with three humps

As a wider range of robustness is required, one may consider a larger number of humps in the PRV. An expansion of the PEI-IS with a single hump or two humps can be made for three humps. To this end, for two design parameters such that $0 \le \epsilon < \delta < 1$, let us define two additional perturbed input shapers as follows:

$$\begin{cases} F_3(s) \triangleq A_1 + A_2 e^{-\tau_d(1-\delta)s} \\ F_4(s) \triangleq A_1 + A_2 e^{-\tau_d(1+\delta)s}. \end{cases} \tag{18}$$

Using these, a PEI-IS (so-called PEI-IS3) can be designed as follows:

$$F_{1234}(s) \triangleq F_1(s) \cdot F_2(s) \cdot F_3(s) \cdot F_4(s). \tag{19}$$

It is noted that the length of shaping period is equal to that of the ZVDDD method. Compared with the EI-IS in Singhose et al.

Table 1
Surface fitting parameters for PEI-IS2 and PEI-IS3.

Shaper	Indices	00	10	01	20	11	02	30	21	12	03
PEI-IS2	p_{ij}	0.1138	0.2118	6.759	0.05636	8.133	−110.6	1.785	17.35	−51.90	840.6
PEI-IS3	p_{ij}	0.1108	−0.02680	4.543	2.720	16.78	−71.60	−8.383	−70.97	−217.3	518.1
	q_{ij}	0.1793	1.362	10.44	−11.13	−39.53	−192.0	44.26	334.1	647.2	1566

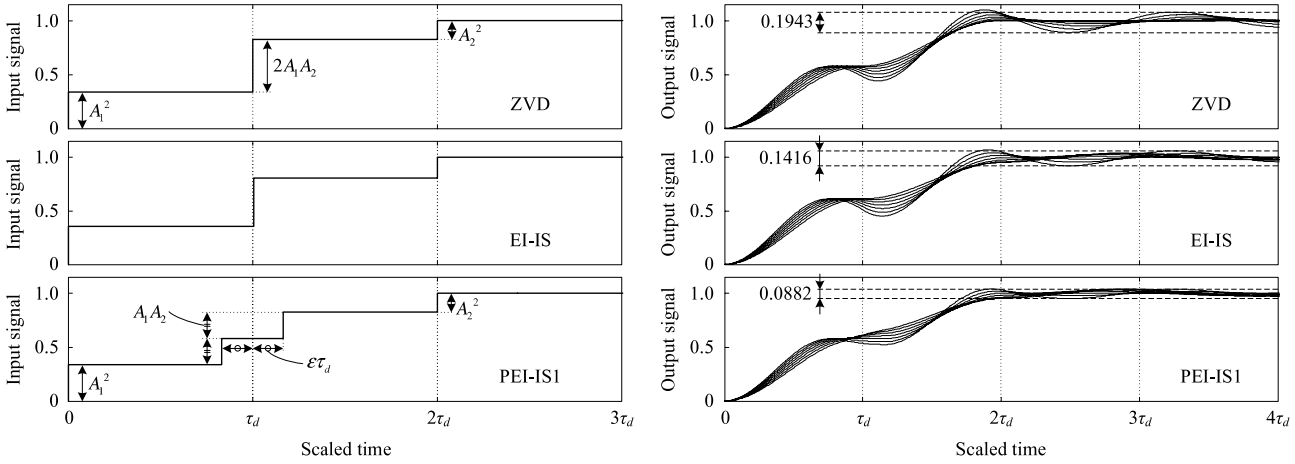

Fig. 4. Responses to the step inputs shaped by the ZVD method, the EI method, and the PEI method with a single hump subjected to a natural frequency variation of up to 30%.

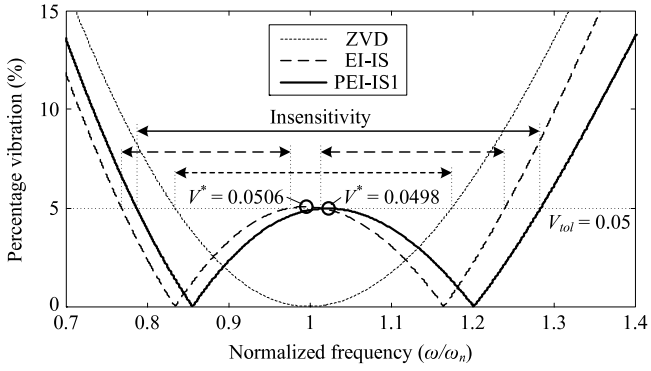

Fig. 5. Definition of insensitivity (a single-hump case).

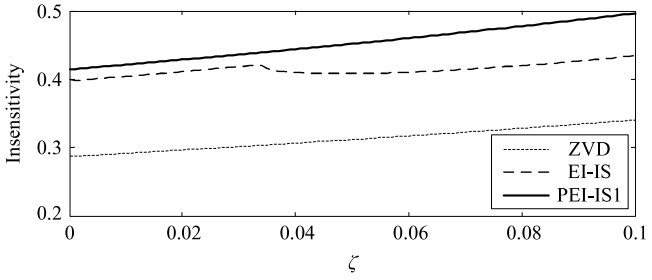

Fig. 6. Comparison of insensitivities under $V_{\text{tol}} = 5\%$ (a single-hump case).

(1997), the proposed method has advantages in design simplicity. That is, (i) the amplitudes of impulses are all fixed by the damping ratio, and (ii) the impulse times are only designed by two design parameters, ϵ and δ.

Similar to the previous cases, the PRV of PEI-IS3 can be expressed by

$$V(\tilde{\omega}) = K^{4\tilde{\omega}} F_{1234}(s_p \tilde{\omega}). \tag{20}$$

The typical shape of the sensitivity curves of PEI-IS3 has three humps, since $V\left(\frac{1}{1+\delta}\right) = V\left(\frac{1}{1+\varepsilon}\right) = V\left(\frac{1}{1-\varepsilon}\right) = V\left(\frac{1}{1-\delta}\right) = 0$. Also, through similar numerical procedures as for the two-hump case, one may have an approximated solution to the design parameters as follows:

$$\begin{cases} \epsilon = [p_{00}, p_{10}, p_{01}, p_{20}, p_{11}, p_{02}, p_{30}, p_{21}, p_{12}, p_{03}] \cdot \varphi^T \\ \delta = [q_{00}, q_{10}, q_{01}, q_{20}, q_{11}, q_{02}, q_{30}, q_{21}, q_{12}, q_{03}] \cdot \varphi^T \end{cases} \tag{21}$$

where the p_{ij} and q_{ij} are summarized in Table 1; they are fitted over $(\zeta, V_{\text{tol}}) \in [0, 0.1] \times [0.01, 0.05]$. It is noted that, in Step (i), we adopted the objective function such that $J_{3h} = (V_\epsilon^* - V_{\text{tol}})^2 + (V_\epsilon^* - V_\delta^*)^2 + (V_\delta^* - V_{\text{tol}})^2$, where V_δ^* is the local maximum at $\tilde{\omega} \in [\frac{1}{1-\epsilon}, \frac{1}{1-\delta}]$. The proposed approximation provides high accuracy within 5.3% mismatch between the peak of the hump and the tolerance over the range $(\zeta, V_{\text{tol}}) \in [0, 0.1] \times [0.01, 0.05]$.

4. Simulation results

Given a sample system $(\zeta, \omega_n) = (0.1, 20\pi)$, in this section, shapers corresponding to single-hump, two-hump, and three-hump cases are designed with $V_{\text{tol}} = 5\%$.

First, the ZVD shaper and the EI-IS and PEI-IS with a single hump (introduced in Section 3.1) are investigated. To test the performance of the shapers in the presence of modeling error, the natural frequency is varied up to 30% from its nominal value. Fig. 4 shows the responses to the shaped step inputs. The time axis of the graph is scaled by the unit τ_d. It can be seen that the residual vibration bounds of the ZVD, EI, and PEI shapers are measured to be 0.1943, 0.1416, and 0.0882, respectively, which proves the notable improvement of robustness of the proposed PEI-IS1.

For rigorous comparison of the envelope of residual vibration, the sensitivity curve is recalled. As shown in Fig. 5, for the sensitivity curves, let us define a measure, the so-called *insensitivity* ($\triangleq \Delta\tilde{\omega}$). $\Delta\tilde{\omega}$ is the range of normalized frequency in which $V(\tilde{\omega}) \le V_{\text{tol}}$ (=0.05). It is noted that, in the case of the EI shaper generated in Singhose et al. (1994), the peak value of the hump exceeds V_{tol}, so the exceeding range is excluded for counting the insensitivity. In this manner, the insensitivities are computed for all $\zeta \in [0, 0.1]$; they are shown in Fig. 6. The figure clearly shows that the proposed PEI-IS1 has better robustness against natural frequency variations than that of ZVD or EI approaches.

Now, the ZVDD shaper, EI-IS, and PEI-IS2 (having two humps) discussed in Section 3.2 are considered. To see the robustness of the

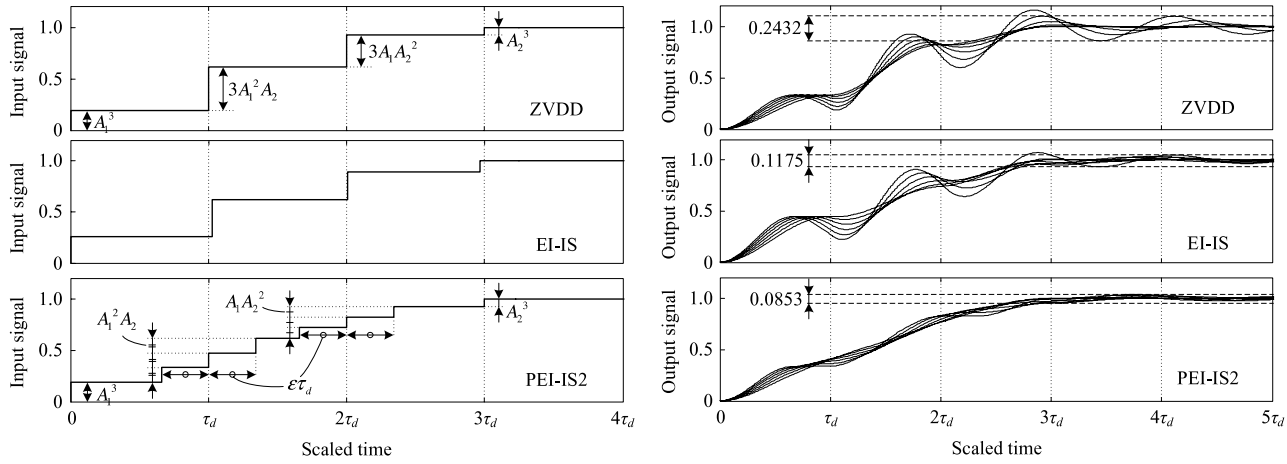

Fig. 7. Responses to the step inputs shaped by the ZVDD method, the EI method, and the PEI method with two humps subjected to a natural frequency variation of up to 50%.

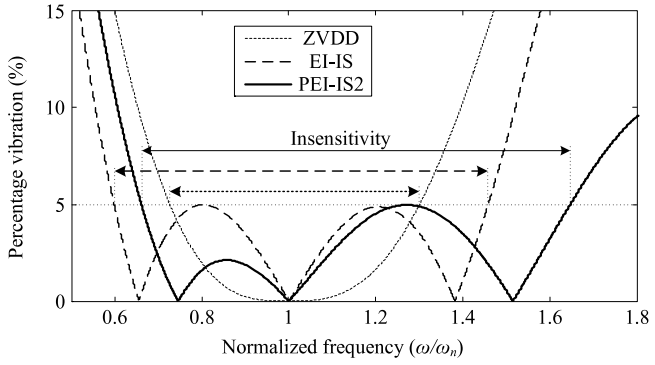

Fig. 8. Definition of insensitivity (two-hump case).

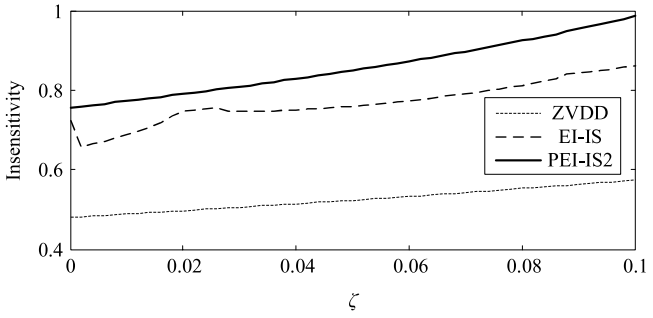

Fig. 9. Comparison of insensitivities under $V_{\text{tol}} = 5\%$ (two-hump case).

shapers, the natural frequency variation is varied up to 50%. Fig. 7 shows the time responses when the shaped inputs are applied to the sample system. PEI-IS2 has more frequent step changes than the others while keeping the same shaping period (i.e., $3\tau_d$). It is apparent that PEI-IS2 suppresses the residual vibration robustly against the natural frequency variations. This fact can be also verified by evaluating the insensitivity, as shown in Figs. 8 and 9. It is observed that the robustness of PEI-IS2 is consistently larger than that of the ZVDD shaper or EI-IS for all $\zeta \in [0, 0.1]$.

Finally, the ZVDDD shaper, EI-IS, and PEI-IS3 having three humps are designed and investigated for the same system. Assuming that the natural frequency varies up to 100% from its nominal value, the time responses to the step input are simulated; they are shown in Fig. 10. PEI-IS3 remarkably reduces the residual vibration subjected to the parameter variation, while keeping the same shaping period as that of the ZVDDD shaper (i.e., $4\tau_d$). The sensitivity curve of PEI-IS3 in Fig. 11 shows significant enhancement of insensitivity, compared with the ZVDDD and EI-IS methods. In particular, the wide insensitive range to natural frequency variation of PEI-IS3 (especially toward high frequency) would be advantageous to suppress the parasitic vibration which may be caused by unmodeled dynamics in a flexible structure. For various nominal values of $\zeta \in [0, 0.1]$, the insensitivities are evaluated and shown in Fig. 12, which proves the robustness compared with the known approaches.

As a remark, the proposed PEI-ISs requiring more impulses than the other methods are advantageous for suppressing not only the residual vibration in the end of the motion but also the *transient vibration* during the motion thanks to the frequent destructive interference of vibrations from the impulses. This can be clearly seen in Figs. 4, 7 and 10 (right), but, for quantitative comparison, let us adopt a measure, namely, the so-called robustness function introduced by Kang (2011) as follows:

$$R = \frac{\int_{t_i}^{t_f} \left(y_{\text{IS}} - y_{\text{rigid}}\right)^2 dt}{\int_{t_i}^{t_f} \left(y_{\text{noIS}} - y_{\text{rigid}}\right)^2 dt}, \tag{22}$$

where y_{noIS} and y_{IS} are the displacements of the flexible mode with and without input shaping under the rigid mode motion represented by y_{rigid}. In (22), t_i and t_f are selected as the first and final times of the shaper impulses to observe the transient response. For the three-hump case, the robustness functions are evaluated under the natural frequency variation and shown in Fig. 13, which shows that the proposed PEI-IS3 has consistently better performance for suppressing the transient vibration than the other approaches. For single-hump and two-hump cases, similar tendencies have been obtained. Similar to the proposed PEI-ISs, there are several approaches to limit the transient vibration in the literature (Singhose, Banerjee, & Seering, 1997; Sung & Singhose, 2008).

Compared with the specified insensitivity input shaper (SI-IS) (Kim & Singhose, 2010; Singhose, Seering, & Singer, 1996; Vaughan, Kim, & Singhose, 2010), the PEI-ISs are advantageous to usability and transient response. The SI-IS which can be generated for any desired level of insensitivity requires optimization, but the PEI-ISs have explicit solutions. Moreover, PEI-ISs having more impulses have better performance for suppressing the transient vibration than the SI-IS under the same insensitivity. However, the shaping period of the SI-IS is shorter than that of the PEI-IS.

5. Conclusion

Robust input shapers were newly proposed based on an impulse-time perturbation approach, the so-called perturbation-based extra-insensitive input shaper (PEI-IS). The percent residual

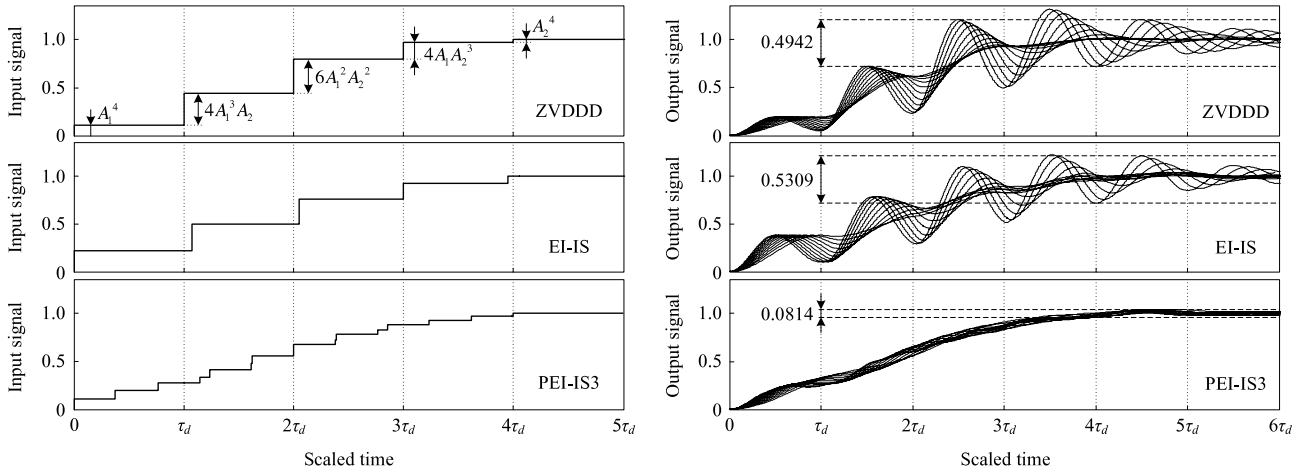

Fig. 10. Responses to the step input shaped by the ZVDDD method, the EI method, and the PEI method with three humps, subjected to a natural frequency variation of up to 100%.

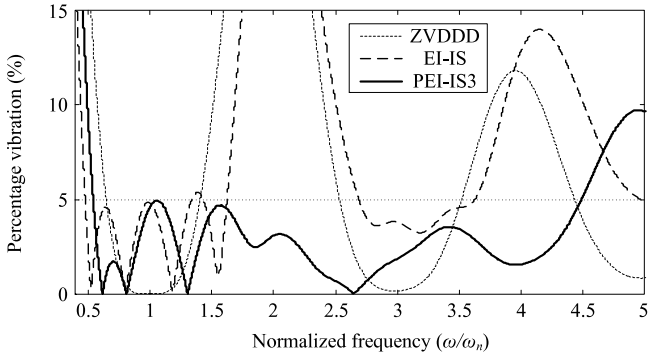

Fig. 11. Sensitivity curves for the ZVDDD shaper, the EI shaper, and the PEI shaper with three humps.

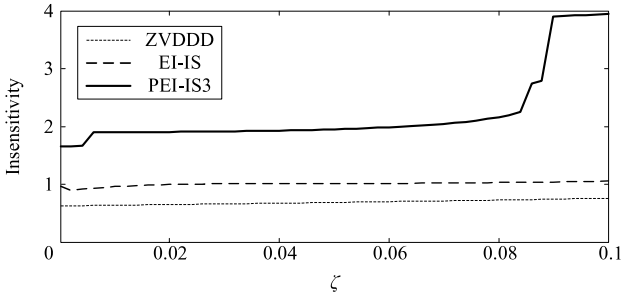

Fig. 12. Comparison of insensitivities under $V_{\text{tol}} = 5\%$ (three-hump case).

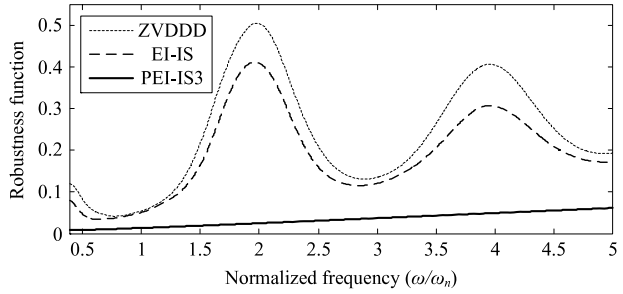

Fig. 13. Robustness functions for the ZVDDD shaper, the EI shaper, and PEI shaper with three humps.

vibration (PRV) of the PEI-IS was represented by the multiplication of transfer functions of perturbed input shapers. This allows the derivation of a closed-form solution to the PEI-IS with a single hump. Furthermore, the idea was extended, with ease, to handle a PEI-IS with two or three humps. Through analysis and simulations, the robustness and advantages of the proposed PEI-ISs were demonstrated.

Acknowledgment

The authors would like to thank Prof. Chul-Ku Kang for his keen insight and outstanding advice.

References

Baumgart, M. D., & Pao, L. Y. (2007). Discrete time-optimal command shaping. *Automatica*, *43*(8), 1403–1409.
Diaz, I. M., Pereira, E., Feliu, V., & Cela, J. J. L. (2010). Concurrent design of multimode input shapers and link dynamics for flexible manipulators. *IEEE/ASME Transactions on Mechatronics*, *15*(4), 646–651.
Ha, C.-W., Rew, K.-H., & Kim, K.-S. (2012). Robust zero placement for motion control of lightly damped systems. *IEEE Transactions on Industrial Electronics*, *60*(9), 3857–3864.
Kang, C.-G. (2011). Performance measure of residual vibration control. *Journal of Dynamic Systems, Measurement, and Control*, *133*(4), 044501.
Kim, D., & Singhose, W. E. (2010). Performance studies of human operators driving double-pendulum bridge cranes. *Control Engineering Practice*, *18*(6), 567–576.
Kozak, K., Singhose, W. E., & Ebert-Uphoff, I. (2006). Performance measures for input shaping and command generation. *Journal of Dynamic Systems, Measurement, and Control*, *128*(3), 731–736.
Meckl, P.H., & Arestides, P.B. (1998). Optimized S-curve motion profiles for minimum residual vibration. In *Proceedings of American control conference, Philadelphia, PA USA* (pp. 2627–2631).
Pao, L.Y., Chang, T.N., & Hou, E. (1997). Input shaper designs for minimizing the expected level of residual vibration in flexible structures. In *Proceedings of American control conference, Albuquerque, NM USA* (pp. 3542–3546).
Pao, L. Y., & Singhose, W. E. (1998). Robust minimum time control of flexible structures. *Automatica*, *34*(2), 229–236.
Park, U. H., Lee, J. W., Lim, B. D., & Sung, Y. G. (2001). Design and sensitivity analysis of an input shaping filter in the *z*-plane. *Journal of Sound and Vibration*, *243*(1), 157–171.
Pereira, E., Trapero, J. R., Diaz, I. M., & Feliu, V. (2009). Adaptive input shaping for manoeuvring flexible structures using an algebraic identification technique. *Automatica*, *45*(4), 1046–1051.
Rew, K.-H., Ha, C.-W., & Kim, K.-S. (2009). A practically efficient method for motion control based on asymmetric velocity profile. *International Journal of Machine Tools and Manufacture*, *49*(7–8), 678–682.
Rew, K.-H., & Kim, K.-S. (2010). A closed-form solution to asymmetric motion profile allowing acceleration manipulation. *IEEE Transactions on Industrial Electronics*, *57*(7), 2499–2506.
Singer, N. C., & Seering, W. P. (1990). Preshaping command inputs to reduce system vibration. *Journal of Dynamic Systems, Measurement, and Control*, *112*(1), 76–82.
Singhose, W. E., Banerjee, A. K., & Seering, W. P. (1997). Slewing flexible spacecraft with deflection-limiting input shaping. *Journal of Guidance, Control, and Dynamics*, *20*(2), 291–298.
Singhose, W. E., Porter, L. J., Tuttle, T. D., & Singer, N. C. (1997). Vibration reduction using multi-hump input shapers. *Journal of Dynamic Systems, Measurement, and Control*, *119*(2), 320–326.
Singhose, W. E., Seering, W. P., & Singer, N. C. (1994). Residual vibration reduction using vector diagrams to generate shaped inputs. *Journal of Mechanical Design*, *116*(2), 654–659.

Singhose, W. E., Seering, W. P., & Singer, N. C. (1996). Input shaping for vibration reduction with specified insensitivity to modeling errors. In *Proceedings of Japan–USA symposium on flexible automation, Boston, MA USA* (pp. 307–313).
Sorensen, K. L., & Singhose, W. E. (2008). Command-induce vibration analysis using input shaping principles. *Automatica*, *44*(9), 2392–2397.
Sung, Y.-G., & Singhose, W. E. (2008). Deflection-limiting commands for systems with velocity limits. *Journal of Guidance, Control, and Dynamics*, *31*(3), 472–478.
Vaughan, J., Kim, D., & Singhose, W. E. (2010). Control of tower cranes with double-pendulum payload dynamics. *IEEE Transactions on Control Systems Technology*, *18*(6), 1345–1358.

Keun-Ho Rew was born in Seoul, Korea, on January 30, 1971. He received his B.S. and M.S. degrees in mechanical engineering and his Ph.D. in aerospace engineering from Korea Advanced Institute of Science and Technology (KAIST), Daejeon, Korea, in 1994, 1996, and 2001, respectively. He was a Senior Engineer with Mirae Industry Company, Ltd., Cheonan, Korea, from 2001 to 2003, and a Chief Engineer with Fine D&C Company, Ltd., from 2003 to 2005. Since 2005, he has been with the Department of Mechanical Engineering, Hoseo University, Asan, Korea, as a Faculty Member. Also, he served as the head of the Department of Robotic Engineering, from 2007 to 2009. His research interests include motion control, robotics, actuation mechanisms, and digital image processing for industrial and rehabilitation robots.

Chang-Wan Ha was born in Busan, Korea, on October 19, 1985. He received his B.S. degree in mechanical engineering from Handong Global University, Pohang, Korea, in 2008, and his M.S. degree in mechanical engineering from KAIST, Daejeon, Korea, in 2010, where he is currently working toward his Ph.D. degree. His research interests include motion control, digital system design for controlled mechatronics, and semiconductor manufacturing equipment.

Kyung-Soo Kim was born in Chungnam, Korea, on March 30, 1973. He received his B.S., M.S., and Ph.D. degrees in mechanical engineering from KAIST, Daejeon, Korea, in 1993, 1995, and 1999, respectively. He was a Chief Researcher with LG Electronics, Inc., from 1999 to 2003, and a DVD Group Manager with STMicroelectronics Company Ltd., from 2003 to 2005. In 2005, he joined the Department of Mechanical Engineering, Korea Polytechnic University, Kyonggi-do, Korea, as a Faculty Member. Since 2007, he has been with the Department of Mechanical Engineering, KAIST. He serves as an associate editor of AUTOMATICA and the Journal of Mechanical Science and Technology. His research interests include digital system design for controlled mechatronics, actuator design, and control theories such as robust control and sliding mode control.